

# Site-specific intravascular ultrasound analysis of remodelling index and calcified necrosis patterns reveals novel blueprints for coronary plaque instability

Scott W. Murray<sup>1,2</sup>, Billal Patel<sup>1</sup>, Rodney H. Stables<sup>1</sup>, Raphael A. Perry<sup>1</sup>, Nicholas D. Palmer<sup>1</sup>

<sup>1</sup>Institute for Cardiovascular Medicine and Science, Liverpool Heart and Chest Hospital, Liverpool, UK; <sup>2</sup>Department of Critical Care Research, University of Liverpool, Liverpool, UK

Correspondence to: Scott W. Murray, Liverpool Heart and Chest Hospital, 14 Thomas Drive, Broadgreen, Liverpool L14 3PE, UK.

Email: scottmurray@doctors.org.uk.

**Aims:** Post-mortem pathological studies have shown that a “vulnerable” plaque is the dominant patho-physiological mechanism responsible for acute coronary syndromes (ACS). One way to improve our understanding of these plaques *in vivo* is by using histological “surrogates” created by intravascular ultrasound derived virtual histology (IVUS-VH). Our aim in this analysis was to determine the relationship between site-specific differences in individual plaque areas between ACS plaques and stable plaques (SP), with a focus on remodelling index and the pattern of calcifying necrosis.

**Methods and results:** IVUS-VH was performed before percutaneous intervention in both ACS culprit plaques (CP) n=70 and stable disease (SP) n=35. A total of 210 plaque sites were examined in 105 lesions at the minimum lumen area (MLA) and the maximum necrotic core site (MAX NC). Each plaque site had multiple measurements made including some novel calculations to ascertain the plaque calcification equipoise (PCE) and the calcified interface area (CIA). CP has greater amounts of positive remodelling at the MLA (RI@MLA): 1.1 ( $\pm$ 0.17) *vs.* 0.95 ( $\pm$ 0.14) (P<0.001); lower values for PCE 30% *vs.* 54% (P<0.001) but a higher CIA 5.38 ( $\pm$ 2.72) *vs.* 3.58 ( $\pm$ 2.26) (P=0.001). These features can provide discriminatory ability between plaque types with area under the curve (AUC) measurements between 0.65-0.86. The cut-off values with greatest sensitivity and specificity to discriminate CP morphologies were: RI @ MLA >1.12; RI @ MAX NC >1.22; PCE @ MLA <47.1%; PCE @ MAX NC <47.3%; CIA @ MLA >2.6; CIA @ MAX NC >3.1.

**Conclusions:** Determining the stage of calcifying necrosis, along with the remodelling index can discriminate between stable and ACS related plaques. These findings could be applied in the future to help detect plaques that have a vulnerable phenotype.

**Keywords:** Intravascular ultrasound; virtual histology; vulnerable plaque; acute coronary syndromes (ACS)

Submitted Jun 12, 2014. Accepted for publication Jul 25, 2014.

doi: 10.3978/j.issn.2223-3652.2014.07.03

View this article at: <http://dx.doi.org/10.3978/j.issn.2223-3652.2014.07.03>

## Introduction

Post-mortem pathological studies have shown that a “vulnerable” plaque is the dominant patho-physiological mechanism responsible for acute coronary syndromes (ACS) (1-3). However, despite this knowledge, we have not yet reached a stage in our diagnostic ability where we are able to predict an event. One way to image plaques *in vivo* is by using histological “surrogates” created by intravascular

ultrasound derived virtual histology (IVUS-VH) (4). IVUS-VH has been validated in human pathological studies and atherectomy specimens and is based upon the analysis of ultrasound backscatter as different plaque components produce a particular spectrum (5-7). The power, amplitude and frequency of the signal undergo de-convolution through a trained classification tree. This process transforms signals into four colour-coded pixels: fibrous (green); fibro-fatty

tissue (light green); necrotic core (red) and dense calcium (white). This has been found to correlate with histopathology and atherectomy specimens (predictive accuracy =87.1%, 87.1%, 88.3%, and 96.5% for fibrous, fibro-fatty, necrotic core, and dense calcium, respectively) (5-7).

Numerous other studies have analysed atherosclerosis with IVUS-VH (8-16). The main focus of these studies has been on conventional parameters and outputs from a standard Virtual Histology (VH) analysis. However, no study has concentrated on remodelling index and the relationship that exists between necrotic core and calcification.

We have focused on this to try and find patterns or “blueprints” that might explain the individual plaque phenotypes seen in ACS.

The process of plaque calcification is incompletely understood and documentation or measurements of calcification patterns are difficult. It is not completely clear what role progressive calcification plays in plaque instability (17-19). Recently, a novel nuclear tracer of active calcification (18F-NaF) has been found to highlight both ruptured and high risk plaques using Positron Emission Computed Tomography (PET CT) (17). The VH analysis of the tracer positive plaques appeared to show more evidence of positive remodelling and micro-calcification.

We therefore examined, in an observational study, culprit plaques (CP) implicated in ACS and stable plaques (SP) responsible for symptomatic angina pectoris. The research aims were:

- (I) To define site-specific differences in atherosclerosis between ACS and SP;
- (II) To “dissect” down, looking for differences in remodelling and calcification patterns at:
  - (i) Minimum lumen area (MLA);
  - (ii) Site of maximum necrotic core content (Max NC).
- (III) To calculate novel markers of vulnerability and/or plaque “blueprints” from frequent patterns or observable recurrent themes.

## Methods

This was a single centre, prospective, observational cohort study that received ethical approval from the Cheshire National Health Service (NHS) ethics committee in the UK. Patients with a Troponin positive ACS diagnosed by a Cardiologist were transferred urgently to our tertiary centre for percutaneous coronary intervention (PCI). These cases were consecutively screened and gave written informed consent to be involved in the study. The main

exclusion criteria were: ST elevation MI; unsuitable anatomy for PCI; left main stem disease; chronic kidney disease; previous PCI in the target vessel and heavily calcified or visibly thrombotic vessels. CP were defined as those meeting electrocardiographic (ECG) criteria for the ACS culprit vessel and where intervention was performed. SP were recruited from patients requiring PCI for progressive symptoms from a known stenotic lesion with failure of medical therapy in an elective setting.

All vessels were studied prior to any percutaneous revascularisation. Imaging of the vessel in each group was undertaken using a phased array catheter (EagleEye catheter, 2.9 F/20 MHz; Volcano Corp). Proximal and distal marker frames were chosen in keeping with a consensus document on how to analyse both IVUS and VH (20). Following administration of Heparin 70 U/KG and a minimum of 1mg of isosorbide dinitrate (ISDN) intra-arterially, the IVUS transducer was advanced beyond the presumed lesion into a clean reference segment. The next distal side-branch was then used as a marker for localisation during IVUS image assessment. The proximal border for image assessment was established in a similar fashion using another side branch or the mouth of the guide catheter. A continuous motorized pull-back at 0.5 mm/s was performed (Volcano R100 pullback device) until the probe had passed the proximal marker. The plaque composition and other analyses were performed by off-line IVUS-VH analysis (S5i Tower and PC VIAS 3.0.394 software; Volcano Corporation) after manual adjustment of border contours by a single individual blinded to the patient details and mode of presentation. Single operator analysis of ACS plaques produces less measurement error as shown in our validation work, which has been previously published (21). This cohort of patients has been taken from the Liverpool IVUS-V-HEART study (22) and a fresh, site-specific plaque area analysis has been undertaken.

### *Methods of detailed plaque analysis using VH*

From this previously published work looking at entire plaques and the volume of plaque components, we have shown that certain measurable factors can help distinguish plaques present in ACS (22). In particular, MLA, plaque burden (PB), necrotic core to dense calcium ratio (NC/DC) and remodelling index (RI) were the most important factors in a multivariate prediction model (22). For this current work we have applied these findings to site-specific, single frame areas within plaques (MLA and MAX NC) to explore

**Table 1** Patient baseline characteristics

Characteristic	ACS (N=70) culprit (CP)	Stable angina (N=35) stable (SP)	P value
Mean age ( $\pm$ SD)	59.2 $\pm$ 11.0	60.1 $\pm$ 7.8	ns
Male, %	73	60	ns
LAD/diagonal	41%	74%	0.03
Circumflex/OM	25%	12%	0.01
Right coronary	34%	14%	0.01
Mean troponin ( $\pm$ SD)	14.8 $\pm$ 27.2	n/a	n/a
Median troponin (IQR)	1.4 (0.1-13.7)	n/a	n/a
Hypertension	51%	59%	ns
Diabetes	24%	18%	ns
Current smoker	54%	57%	ns
Hypercholesterolaemia	60%	52%	ns
Family history	70%	65%	ns
Chronic kidney disease	3%	1%	ns
Previous MI	16%	7%	0.02

ACS, acute coronary syndromes; SP, stable plaques; CP, culprit plaques; OM, obtuse marginal; IQR, interquartile range; MI, myocardial infarction; n/a, not applicable; ns, non significant.

in more detail the relationship between remodelling, necrosis and calcification. We calculated (NC + DC/DC) area to quantify mathematically a surrogate for the amount of interfacial connection between NC and DC (spottier calcification). We have called this measurement the calcified interface area (CIA). Also, DC/NC area  $\times$ 100 was calculated as a representation of the calcification that has developed respective to the necrotic core; this has been given the term plaque calcification equipoise (PCE). A single previous study has defined micro-calcification as being evidence of "spotty" calcification on three frames or more with no evidence of acoustic shadowing behind the calcium (17). However, we feel that calculating the PCE and CIA provides a more continuous and reproducible way to define the relationship between calcium and necrosis. The remodelling index was defined as the ratio between the external elastic membrane cross-sectional area of the specific site (Max NC or MLA) and the average of the proximal and distal reference regions in the same vessel. The maximum necrotic core frame (MAX NC) was defined as the frame with the highest percentage of necrotic core on a single frame within the culprit lesion complex. The

remodelling index was defined by calculating the ratio of the EEM area at the chosen site (MAX NC/MLA) divided by the sum of EEM area at the best clean proximal reference site and best clean distal reference site/2. These reference sites must have been within 10 mm and within any distal or proximal main side branches.

### Statistics and power calculation

To ensure significant power was available for this sub-study, a post-hoc analysis was made using results for CIA. The mean for one group was 3.58 ( $\pm$ 2.26) and for the other 5.38 ( $\pm$ 2.71). For an Alpha of 0.05 over 105 plaque sites, the power to detect a statistical difference was calculated at 94.8%. Continuous variables are expressed as means  $\pm$  standard deviation (SD). On comparing plaques sites a student's *t*-test was used when the data was normally distributed, however if variances were unequal or a two sided F test was significant a Mann-Whitney U test was performed to ensure statistical significant was met for median values. A P value of <0.05 was taken as indicating a statistically significant result. Receiver operator characteristics were used to test the discriminatory ability of certain plaque variables, this was done with the binary classification: 1= CP ACS culprit/troponin positive; 0= SP. Plaque variables that have shown statistical differences between these groups were also explored by simple linear regression to determine any correlation.

### Results

Two hundred and thirty eight patients were approached consecutively after urgent ACS transfer and case note review. Seventeen patients refused to participate and two hundred and twenty one were formally consented and enrolled before angiography. One hundred and fifty one had to be excluded after angiography due to fulfilment of various exclusion criteria. The majority of exclusions (90%) were due to the presence of surgical disease and/or heavy thrombus burden, tight lesion (IVUS unlikely to cross) with reduced TIMI flow in the culprit vessel. Seventy culprit lesions in ACS patients were studied and analysed successfully with IVUS-VH. A further thirty five culprit lesions from stable angina patients undergoing PCI (guided by IVUS) were analysed separately, giving a total patient cohort of one hundred and five. The patient characteristics are seen in *Table 1*.

Following the analysis of two separate sites (MAX NC and MLA) in each individual plaque (n=2 $\times$ 70 CP and n=2 $\times$ 35 SP);

**Table 2** Comparison of sites within a stable angina plaque (n=70)

Variables	Plaque at maximum necrotic core site (MAX NC)	Plaque at minimum lumen area site (MLA)	P value
Lumen area	6.04 ( $\pm$ 2.97)	3.61 ( $\pm$ 1.34)	<0.001
Plaque burden, %	59	68	0.004
NC/DC	2.57 ( $\pm$ 2.25)	2.74 ( $\pm$ 2.82)	0.79 (ns)
Remodelling index	1.1 ( $\pm$ 0.17)	0.95 ( $\pm$ 0.14)	<0.001
Calcium interface area (CIA)	3.58 ( $\pm$ 2.26)	2.36 ( $\pm$ 1.07)	0.005
Plaque calcification equipoise (PCE), %	54	56	0.68 (ns)

DC, dense calcium; ns, non significant.

**Table 3** Comparison of sites within an ACS plaque (n=140)

Variables	Plaque at maximum necrotic core site (MAX NC)	Plaque at minimum lumen area site (MLA)	P value
Lumen area	5.93 ( $\pm$ 2.67)	2.98 ( $\pm$ 1.27)	<0.001
Plaque burden, %	66	79	<0.001
NC/DC	4.38 ( $\pm$ 2.72)	3.46 ( $\pm$ 3.48)	0.08 (ns)
Remodelling index	1.34 ( $\pm$ 0.18)	1.20 ( $\pm$ 0.13)	<0.001
Calcium interface area (CIA)	5.38 ( $\pm$ 2.72)	4.33 ( $\pm$ 3.61)	0.001
Plaque calcification equipoise (PCE), %	30	43	0.004

ACS, acute coronary syndromes; DC, dense calcium; ns, non significant.

**Table 4** Comparison of MAX NC site in both stable and ACS plaques (n=105)

Variables	Plaque at maximum necrotic core site (MAX NC)—stable	Plaque at maximum necrotic core site (MAX NC)—ACS	P value
Lumen area	6.04 ( $\pm$ 2.97)	5.93 ( $\pm$ 2.67)	0.85
Plaque burden, %	59	66	0.012
NC/DC	2.57 ( $\pm$ 2.25)	4.38 ( $\pm$ 2.72)	<0.001
Remodelling index	1.1 ( $\pm$ 0.17)	1.34 ( $\pm$ 0.18)	<0.001
Calcium interface area (CIA)	3.58 ( $\pm$ 2.26)	5.38 ( $\pm$ 2.72)	0.001
Plaque calcification equipoise (PCE), %	54	30	<0.001

ACS, acute coronary syndromes; DC, dense calcium.

a total of n=210 separate plaque sites were analysed and measured. In general, more left anterior descending arteries were examined in the stable group with more right coronary and circumflex arteries being involved in the ACS group. More ACS patients had suffered a previous myocardial event. An overview of the focused IVUS and VH comparisons for each plaque type and site is present in *Tables 2-5*. *Table 2* shows that in SP, despite the obvious differences in lumen area [MAX NC 6.04 ( $\pm$ 2.97) *vs.* MLA 3.61 ( $\pm$ 1.34)

mm], there remains a substantial plaque burden at the MAX NC site (59%). Although plaque burden is somewhat greater at the MLA (68%), the lumen is preserved at the MAX NC site and this appears to be accommodated by a greater amount of positive remodelling [1.1 ( $\pm$ 0.17) *vs.* 0.95 ( $\pm$ 0.14)]. The MLA point of a stable plaque is more likely to display negative remodelling [RI 0.95 ( $\pm$ 0.14)]. Also, each of these individual plaque sites appears to have similar values for basic NC/DC ratios [2.57 ( $\pm$ 2.25) *vs.* 2.74 ( $\pm$ 2.82), P=ns].

**Table 5** Comparison of MLA site in both stable and ACS plaques (n=105)

Variables	Plaque at maximum necrotic core site (MAX NC)—stable	Plaque at maximum necrotic core site (MAX NC)—ACS	P value
Lumen area	3.61 (±1.34)	2.98 (±1.27)	0.021
Plaque burden, %	68	79	<0.001
NC/DC	2.74 (±2.82)	3.46 (±3.48)	0.26
Remodelling index	0.95 (±0.14)	1.20 (±0.13)	<0.001
Calcium interface area (CIA)	2.36 (±1.07)	4.33 (±3.61)	<0.001
Plaque calcification equipoise (PCE) %	56	43	0.068

ACS, acute coronary syndromes; DC, dense calcium; ns, non significant.

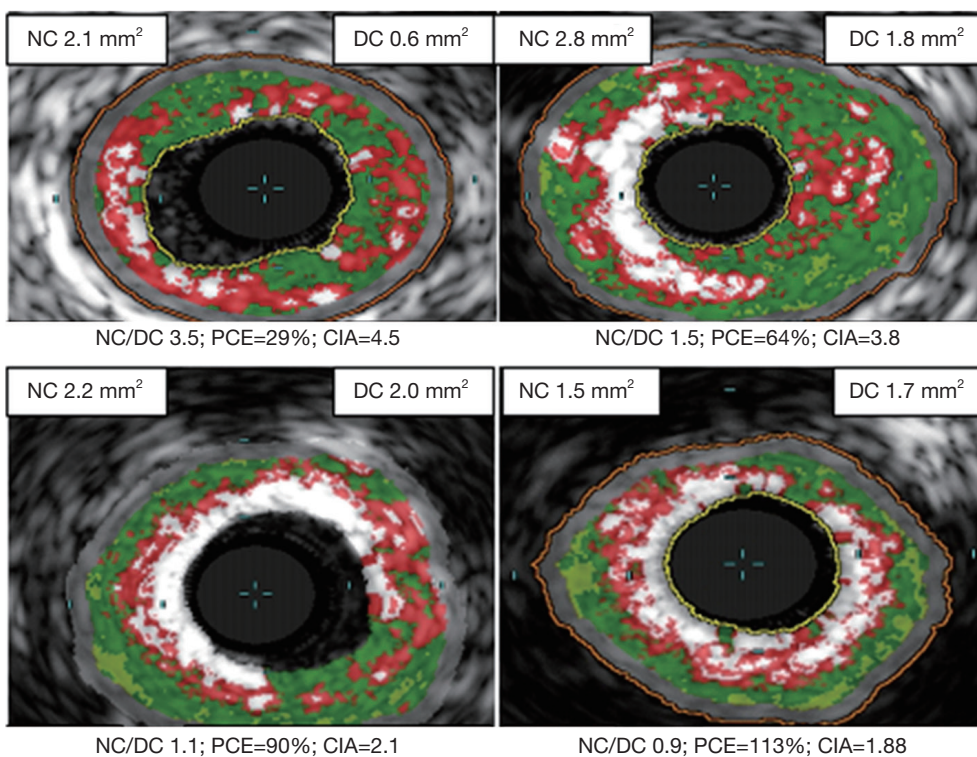


**Figure 1** Virtual Histology evolution of plaque from primitive necrosis and spotty calcium through to calcium arcs. Each stage shows values for NC/DC ratio. PCE, plaque calcification equipoiseand; CIA, calcified interface area; NC/DC, necrotic core to dense calcium ratio.

However, the actual pattern of calcification differs at the MAX NC site, having a greater CIA [MAX NC 3.58 (±2.26) vs. MLA 2.36 (±1.07), P<0.001]. Table 3 shows the results for ACS CP and interestingly a similar pattern emerges. However, these plaques appear to have less calcification overall and greater amounts of positive remodelling both at the MLA and MAX NC site, when compared to stable plaque disease. Moreover, the MAX NC site within a culprit plaque has the greatest amount of positive remodelling

across all the plaque types [RI 1.20 (±0.13) vs. 1.34 (±0.18), P<0.001].

On direct comparison between CP and SP at these specific points in the plaque (Tables 4 and 5) we can again observe important statistical differences. These results, demonstrated visually in Figure 1, explain the intricate pathological changes that are seen in plaques, at different stages of atherosclerosis. Graphical explanations of the results (as an aid to comprehension) are displayed in Figures 2-4.

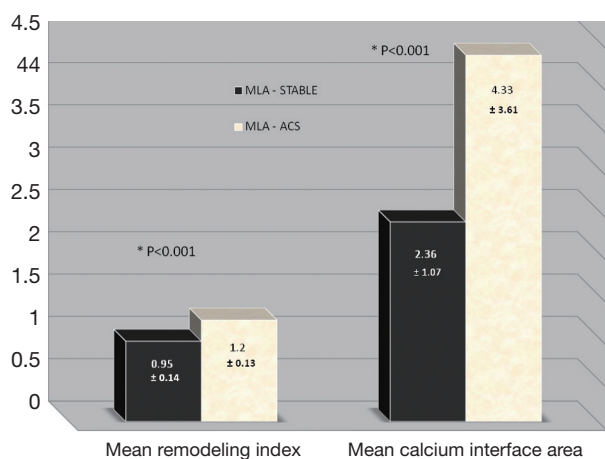


**Figure 2** Histogram showing significant differences in remodelling index and calcified interface area at the minimum lumen area (MLA) in both ACS and stable plaques. ACS, acute coronary syndromes.

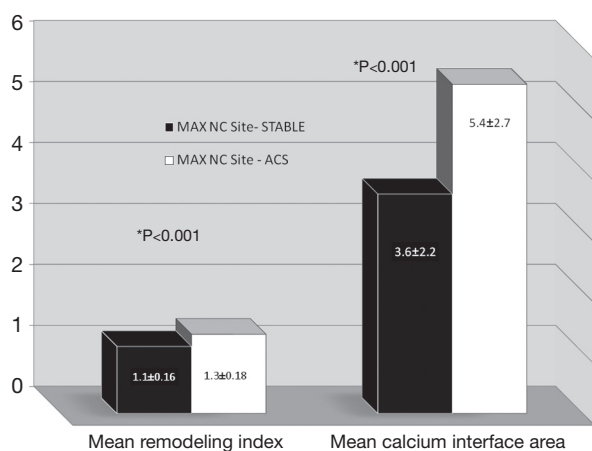


**Figure 3** Histogram showing significant differences in remodelling index and calcified interface area at the maximum necrotic core (MAX NC) site in both ACS and stable plaques. ACS, acute coronary syndromes.

These statistical differences have been explored using ROC analysis to look for discriminatory ability. This is shown in *Figures 5* and *6*. Although the area under the curve (AUC) and sensitivity/specificity vary somewhat (0.86-0.65 and 97-51%) the best cut-off values to determine blueprints for “culprit plaque-like” morphologies are: RI @ MLA >1.12; RI @ MAX NC >1.22; PCE @ MLA <47.1%; PCE @ MAX NC <47.3%; CIA @ MLA >2.6; CIA @ MAX NC >3.1.

Analysis of the data, to look for correlations between remodelling index and patterns of atherosclerosis/

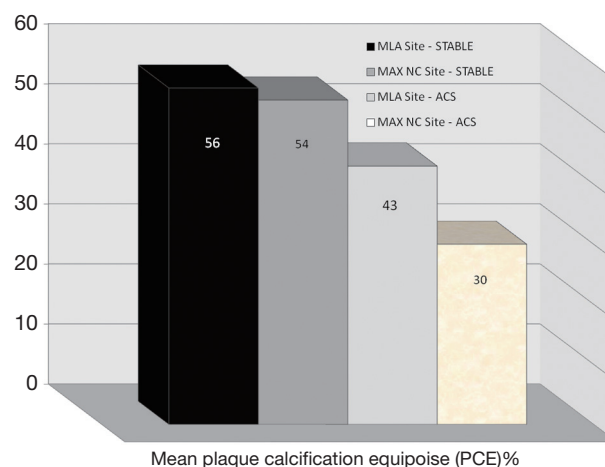


**Figure 4** Histogram showing means PCE across the major plaque sites in both ACS and stable plaques. This displays the change in percentage calcification between different clinical presentations. PCE, plaque calcification equipoise; ACS, acute coronary syndromes.

calcification, shows the following:

- (I) No significant direct correlation between remodelling index and PCE. However, there is a weak negative trend ( $P < 0.09$ ) in SP; as plaque calcification increases the remodelling index decreases. This may be a signal towards some contraction of the vessel size as calcification increases (*Figure 7*);
- (II) A trend ( $P = 0.07$ ) in SP towards a positive correlation between CIA and remodelling index. This may be a signal that spotty calcification and positive remodelling are linked (*Figure 7*);
- (III) A statistically significant negative correlation between CIA and PCE. This makes sense as calcification increases, spotty calcification decreases. This relationship is shown in *Figures 8* and *9*.

## Discussion

New blueprints to help assess plaque vulnerability, before a fatal event, are urgently called for. We have presented a series of novel observational virtual histology IVUS findings gathered from the analysis of 210 plaque sites across the spectrum of stable and unstable coronary disease. This reveals (in ACS CP) the striking feature of positive remodelling and primitive “spotty” calcification within the necrotic core (RI; CIA; PCE). We have also shown via our calculations that stable phenotypes tend to have

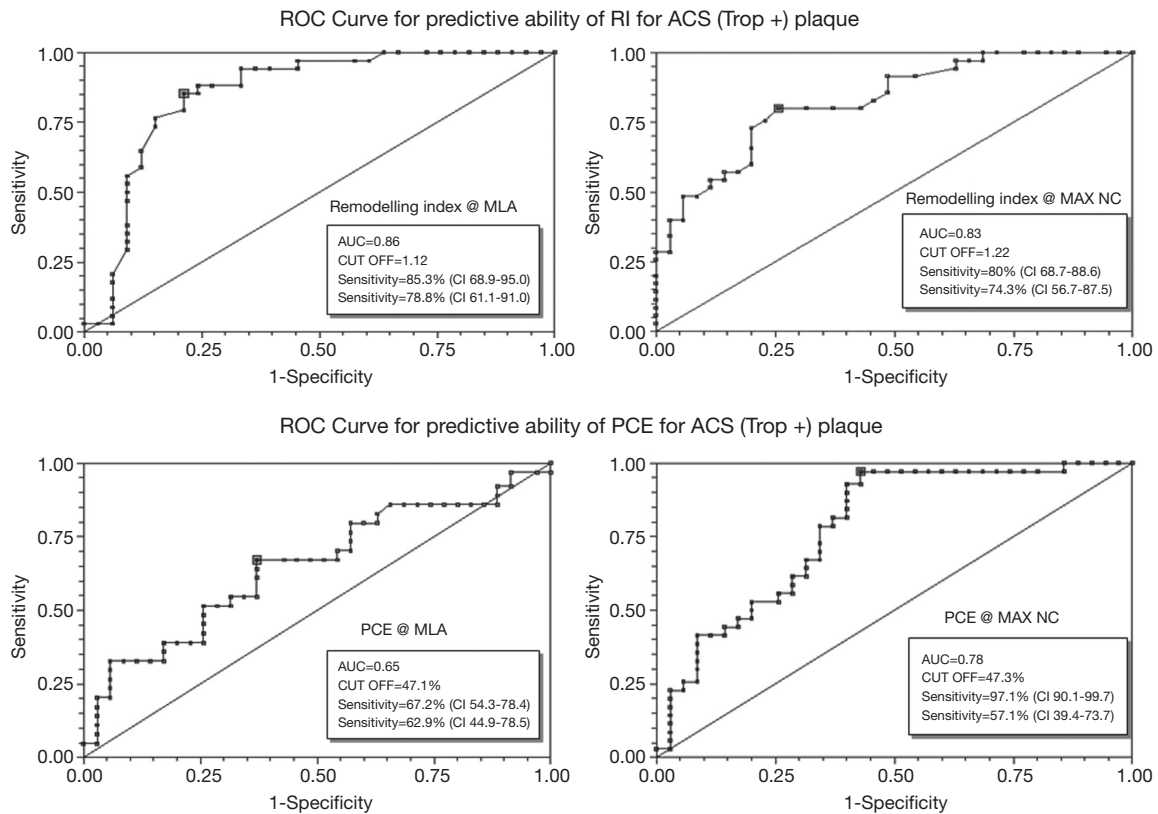


**Figure 5** ROC curves showing discriminatory ability of remodelling index and PCE to determine culprit ACS plaques. PCE, plaque calcification equipoiseand; ACS, acute coronary syndromes; ROC, receiver operating characteristic.

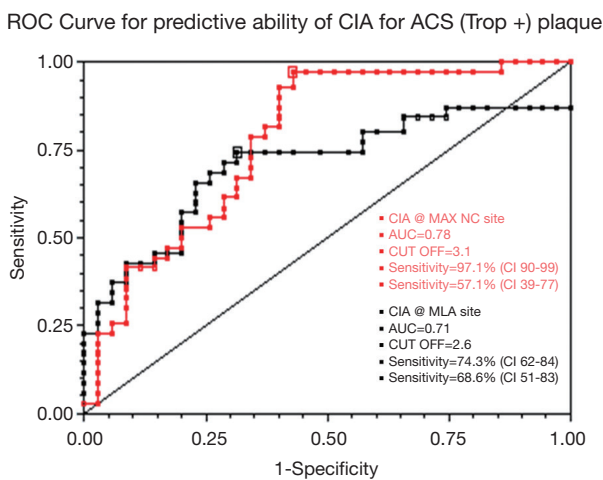


**Figure 6** ROC curve for CIA showing good discriminatory ability for ACS plaques using this measurement obtained both at MLA and MAX NC sites. CIA, calcified interface area; ACS, acute coronary syndromes; MLA, minimum lumen area; MAX NC, maximum necrotic core.

a greater extent of calcification as measured by the PCE (>47%). This cut off value (close to 50% calcification) could be the “equipoise point” where a plaque is in calcific transition from a “spotty-type” to a more organised “arc-like” form, hence the term PCE. Also, through calculating the CIA, we have shown that potentially different patterns of calcification can exist despite similar values for NC, DC, NC/DC ratio or PCE. This has been evident when comparing MAX NC and MLA sites within a stable plaque and also when comparing the MLA point of a culprit ACS plaque (CIA >3) with that of a stable plaque (CIA <3).

Previously, the NC/DC ratio on VH analyses has been shown to correlate with risk factors for sudden cardiac death and high risk ACS presentations (23,24). With regard to the process and role of plaque calcification, it is interesting to discuss this based on a “friend or foe” analogy. Coronary calcium correlates with plaque burden (24,25) but its effect on plaque instability is less evident. Beckman *et al.* (26) demonstrated that the maximal arc of calcium decreased

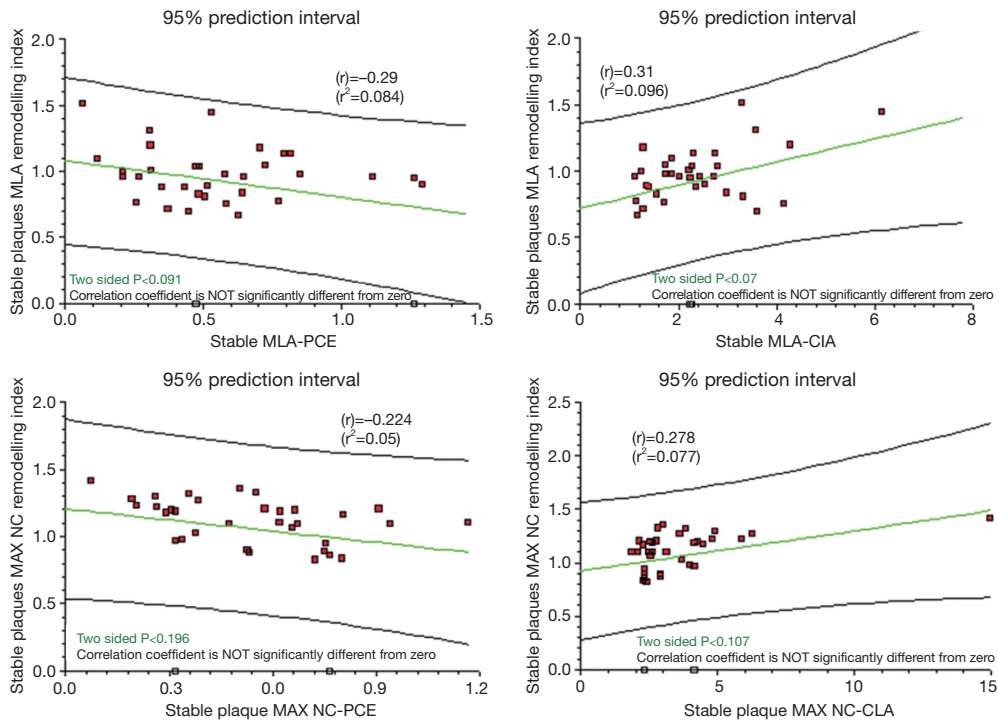


**Figure 7** Scatter plots of linear regression looking for a correlation between Remodelling Index and both PCE and CIA. Weak trends are seen at stable plaque MLA. PCE, plaque calcification equipoiseand; CIA, calcified interface area; MLA, minimum lumen area.

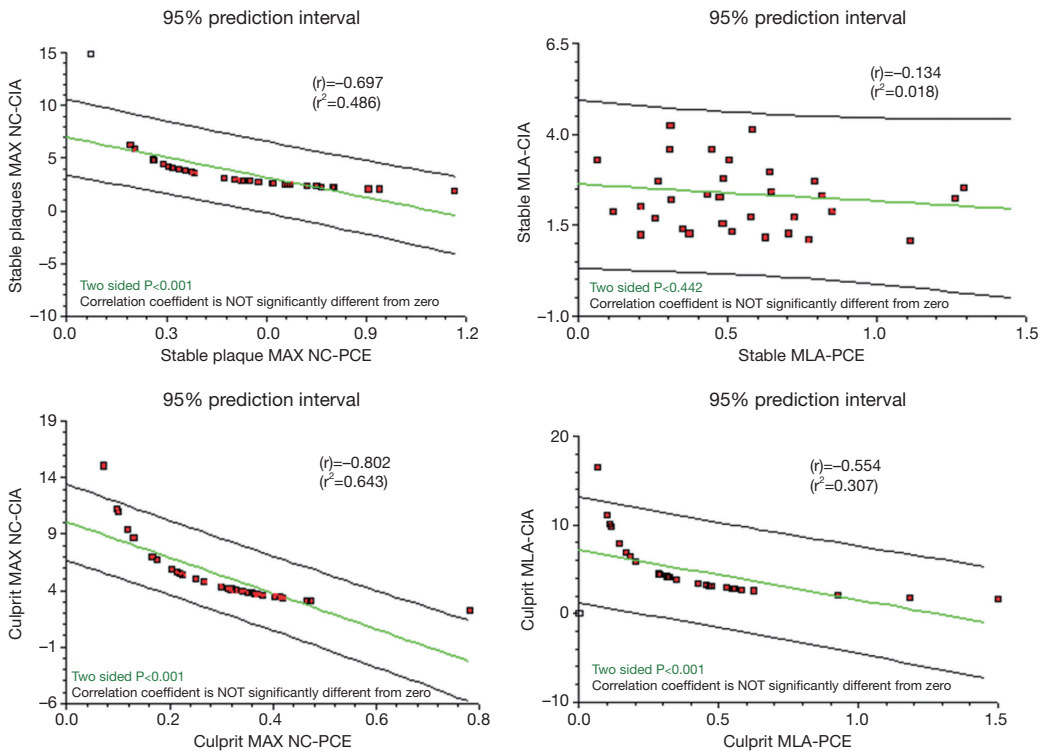


**Figure 8** Scatter plots of linear regression showing a confirmed correlation between CIA and PCE in both stable and ACS plaques. CIA, calcified interface area; PCE, plaque calcification equipoiseand; ACS, acute coronary syndromes.



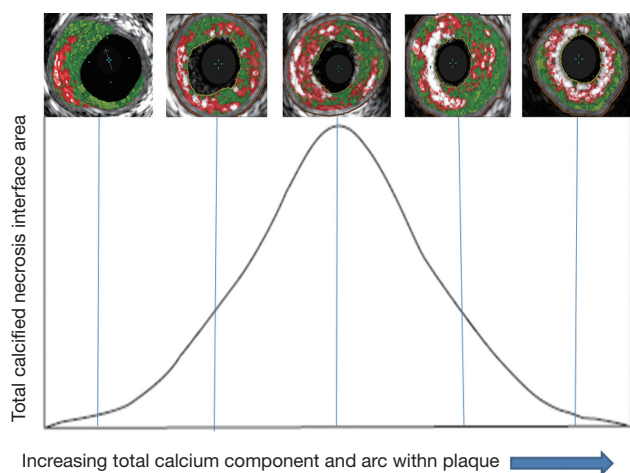


**Figure 9** Graphical representation of the “bell curve theory” relationship between increasing calcium within a lesion and the interfacial area between calcium and necrosis as calcium coalesces.

progressively from patients with stable angina ( $91^{\circ}\pm 10^{\circ}$ ), to those with unstable angina ( $59^{\circ}\pm 8^{\circ}$ ) and finally to those with myocardial infarction ( $49^{\circ}\pm 11^{\circ}$ ,  $P=0.014$ ). Missel *et al.* (23) reported that the average number of calcium deposits (within an arc of  $90^{\circ}$ ) decreased progressively in patients with acute myocardial infarction, compared with unstable angina and those with stable angina. Calcium deposits were also longer in patients with stable angina. Fujii *et al.* (24) showed that ruptured plaques also had quantitatively less calcium but a larger number of small calcium deposits when compared with non-ruptured plaques. It appears that primitive spots of calcification within the necrotic core may be the dangerous foe but as calcification progresses there is a tipping point where it may conversely have a stabilising effect. The individual nuances behind these previous findings can again be explained by our calculations of CIA and PCE (Figures 1 and 9). As the PCE increases beyond 50% and the CIA falls below 4, a certain amount of “plaque contraction” appears to occur as the necrotic core is replaced by calcification. The vessel remodelling in SP with these features is more negative and a trend towards this has been shown on linear regression (Figure 8). This is in keeping with multiple previous analyses highlighting that positive remodelling is more prevalent in acute coronary syndrome plaques (3,10,11,17,22). We deliberately avoided classifying plaques into groups by VH appearance (VH-TCFA/ThCFA/FA etc.) as this has been shown to be plagued by variability errors even between experienced operators (27).

It could be speculated that the development of primitive

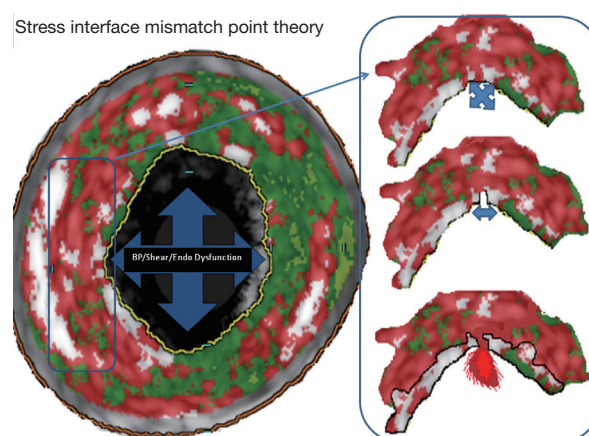


**Figure 10** Virtual Histology explanation of the SIMPS, stress interface mismatch point theory of plaque instability, trigger and rupture based upon evidence from biomechanics and finite element analysis. SIMPS, stress interface mismatch points.

calcification, starting as small “spotty” islands in a sea of necrotic core, is the active process highlighted by  $^{18}\text{F-NaF}$  on PET CT (17) and therefore there must be a rational explanation for the increased risk of these plaques to rupture and cause events.

As an explanation for this, previous biomechanical studies suggest that at the interface between a solid impurity (calcium) and a softer compound (necrosis), the large divergence in material resistance creates local strain concentrations at the poles of the impurity (28-35). Theoretically, should the stress placed on these areas change suddenly, via known plaque rupture triggers, such as increases in blood pressure or localised vasomotor function (sympathetic stimulation), then subsequent tissue de-bonding could occur, separating these tissues and precipitating plaque fissuring/rupture. We have suggested a plausible theory that these points (when seen at the luminal surface/cap) could be called “stress interface mismatch points (SIMPS)” (Figure 10). The prevalence of these sites within a plaque is difficult to define accurately with IVUS-VH. However, we have attempted to infer the presence of this more primitive spotty calcification through the calculation of our two novel markers (PCE and CIA). As previously discussed, as plaque calcification makes progress to theoretically “heal” or stabilise the necrotic core (PCE and CIA). This decreases the prevalence of SIMPS between the calcium speckles, as the intermediary necrotic core is replaced by calcium fusing. A future study may be warranted to explore this in more detail, at the luminal surface, with

optical coherence tomography analysis or finite element analysis (FEA).

In further support of this observational theory for plaque vulnerability/rupture, biomechanical studies using FEA models appear to confirm that micro-calcifications can alter the maximal principal stress by up to 32% (31-33). According to the science of linear elastic fracture mechanics, if a system consisting of two edge-bonded wedges of different materials is considered, a stress-singularity occurs at the vertex of the bi-material interface (34). The existence of these “stress-singularities” means that micro-failure processes can occur at the interfaces, leading to crack initiation and propagation (described in *Figure 10*).

### Limitations

This is a single centre, observational study with the inherent limitations of this design. Our theory is observational and experimental in nature and is built upon the detailed scrutiny of both the IVUS and VH images at each individual plaque frame. Although efforts were made to blind the analysing operator to the presentation type, it is occasionally clear when a plaque is a culprit, due to the presence of thrombus and plaque rupture. This is a potential source of bias. Analysis of high-risk ACS CP required interrogation of IVUS images containing rupture cavities and thrombus at varying stages of progression and therefore we followed previously published guidance by including thrombus (when seen) in the plaque analysis where possible (20). This can be difficult and previous studies have shown a difference between independent IVUS-VH measurements and measurements performed in a core-lab facility (35,36). However, we have published our magnitude of measurement variability in high risk ACS plaques, following a previous in-depth study (19). The inclusion of ratio scores and percentages where DC and NC are involved does merit some discussion as previously in the literature the impact of dense calcium measurement on necrotic core coding from VH has been investigated (37,38). It has previously been shown on some analyses (38) that dense calcium in VH analysis begets the identification of necrotic core behind the calcium signal. Although this is certainly observed in some situations (heavy calcium with signal drop out), it previously did not statistically influence our volume measurements (21). VH is a crude surrogate or “window” to the true plaque histopathology (as the algorithm was built around a single pathologist’s interpretation of “calcifying necrosis”). However, in

support of VH, a recent analysis by the Cambridge group comparing VH to conventional histology (39) revealed that there still appears to be reasonably good diagnostic accuracy for calcified plaque components (92%).

### Conclusions

Intravascular ultrasound can help us characterise plaque remodelling and calcification patterns. From this we have found different morphologies in site-specific areas between stable and ACS presentations. Determining the stage of calcification using the calculations of PCE and CIA, along with the remodelling index can discriminate between plaque types. These findings could be applied in future studies to investigate plaques that may be more prone to rupture.

### Acknowledgements

*Funding:* Liverpool Heart and Chest Hospital, Johnson Interventional Cardiology Research Fellowship.

*Disclosure:* The authors declare no conflict of interest.

### References

1. Falk E, Shah PK, Fuster V. Coronary plaque disruption. *Circulation* 1995;92:657-71.
2. Virmani R, Burke AP, Farb A. Sudden cardiac death. *Cardiovasc Pathol* 2001;10:211-8.
3. Virmani R, Kolodgie FD, Burke AP, et al. Lessons from sudden coronary death: a comprehensive morphological classification scheme for atherosclerotic lesions. *Arterioscler Thromb Vasc Biol* 2000;20:1262-75.
4. Sawada T, Shite J, Garcia García HM, et al. Feasibility of combined use of intravascular ultrasound radiofrequency data analysis and optical coherence tomography for detecting thin-cap fibroatheroma. *Eur Heart J* 2008;29:1136-46.
5. Nasu K, Tsuchikane E, Katoh O, et al. Accuracy of in vivo coronary plaque morphology assessment: a validation study of in vivo virtual histology compared with in vitro histopathology. *J Am Coll Cardiol* 2006;47:2405-12.
6. Van Herck J, De Meyer G, Ennekens G, et al. Validation of in vivo plaque characterisation by virtual histology in a rabbit model of atherosclerosis. *EuroIntervention* 2009;5:149-56.
7. Rodriguez-Granillo GA, Garcia-Garcia HM, Mc Fadden EP, et al. In vivo intravascular ultrasound-derived thin-cap fibroatheroma detection using ultrasound radiofrequency

- data analysis. *J Am Coll Cardiol* 2005;46:2038-42.
8. Calvert PA, Obaid DR, O'Sullivan M, et al. Association between IVUS findings and adverse outcomes in patients with coronary artery disease: the VIVA (VH-IVUS in Vulnerable Atherosclerosis) Study. *JACC Cardiovasc Imaging* 2011;4:894-901.
  9. Stone GW, Maehara A, Lansky AJ, et al. A prospective natural-history study of coronary atherosclerosis. *N Engl J Med* 364 2011 226-35.
  10. García-García HM, Goedhart D, Schuurbiens JC, et al. Virtual histology and remodelling index allow in vivo identification of allegedly high-risk coronary plaques in patients with acute coronary syndromes: a three vessel intravascular ultrasound radiofrequency data analysis. *EuroIntervention* 2006;2:338-44.
  11. Hong MK, Mintz GS, Lee CW, et al. Comparison of virtual histology to intravascular ultrasound of culprit coronary lesions in acute coronary syndrome and target coronary lesions in stable angina pectoris. *Am J Cardiol* 2007;100:953-9.
  12. Hong MK, Mintz GS, Lee CW, et al. A three-vessel virtual histology intravascular ultrasound analysis of frequency and distribution of thin-cap fibroatheromas in patients with acute coronary syndrome or stable angina pectoris. *Am J Cardiol* 2008;101:568-72.
  13. Qian J, Maehara A, Mintz GS, et al. Relation between individual plaque components and overall plaque burden in the prospective, multicenter virtual histology intravascular ultrasound registry. *Am J Cardiol* 2009;104:501-6.
  14. Rodriguez-Granillo GA, McFadden EP, Valgimigli M, et al. Coronary plaque composition of nonculprit lesions, assessed by in vivo intracoronary ultrasound radio frequency data analysis, is related to clinical presentation. *Am Heart J* 2006;151:1020-4.
  15. Surmely JF, Nasu K, Fujita H, et al. Coronary plaque composition of culprit/target lesions according to the clinical presentation: a virtual histology intravascular ultrasound analysis. *Eur Heart J* 2006;27:2939-44.
  16. Nakamura T, Kubo N, Funayama H, et al. Plaque characteristics of the coronary segment proximal to the culprit lesion in stable and unstable patients. *Clin Cardiol* 2009;32:E9-12.
  17. Joshi NV, Vesey AT, Williams MC, et al. 18F-fluoride positron emission tomography for identification of ruptured and high-risk coronary atherosclerotic plaques: a prospective clinical trial. *Lancet* 2014;383:705-13.
  18. Ehara S, Kobayashi Y, Yoshiyama M, et al. Spotty calcification typifies the culprit plaque in patients with acute myocardial infarction: an intravascular ultrasound study. *Circulation* 2004;110:3424-9.
  19. Fujii K, Carlier SG, Mintz GS, et al. Intravascular ultrasound study of patterns of calcium in ruptured coronary plaques. *Am J Cardiol* 2005;96:352-7.
  20. García-García HM, Mintz GS, Lerman A, et al. Tissue characterisation using intravascular radiofrequency data analysis: recommendations for acquisition, analysis, interpretation and reporting. *EuroIntervention* 2009;5:177-89.
  21. Murray SW, Stables RH, Hart G, et al. Defining the magnitude of measurement variability in the virtual histology analysis of acute coronary syndrome plaques. *Eur Heart J Cardiovasc Imaging* 2013;14:167-74.
  22. Murray SW, Stables RH, Garcia-Garcia HM, et al. Construction and validation of a plaque discrimination score from the anatomical and histological differences in coronary atherosclerosis: the Liverpool IVUS-V-HEART (Intra Vascular UltraSound-Virtual-Histology Evaluation of Atherosclerosis Requiring Treatment) study. *EuroIntervention* 2014. [Epub ahead of print].
  23. Missel E, Mintz GS, Carlier SG, et al. Necrotic Core and its Ratio to dense calcium are predictors of high-risk non ST elevation acute coronary syndromes. *Am J Cardiol* 2008;101:573-8.
  24. Missel E, Mintz GS, Carlier SG, et al. In vivo virtual histology intravascular ultrasound correlates of risk factors for sudden coronary death in men: results from the prospective, multi-centre virtual histology intravascular ultrasound registry. *Eur Heart J* 2008;29:2141-7.
  25. Maehara A, Mintz GS, Bui AB, et al. Morphologic and angiographic features of coronary plaque rupture detected by intravascular ultrasound. *J Am Coll Cardiol* 2002;40:904-10.
  26. Beckman JA, Ganz J, Creager MA, et al. Relationship of clinical presentation and calcification of culprit coronary artery stenoses. *Arterioscler Thromb Vasc Biol* 2001;21:1618-22.
  27. Obaid DR, Calvert PA, McNab D, et al. Identification of coronary plaque sub-types using virtual histology intravascular ultrasound is affected by inter-observer variability and differences in plaque definitions. *Circ Cardiovasc Imaging* 2012;5:86-93.
  28. Hoshino T, Chow LA, Hsu JJ, et al. Mechanical stress analysis of a rigid inclusion in distensible material: a model of atherosclerotic calcification and plaque vulnerability *Am J Physiol Heart Circ Physiol* 2009;297:H802-10.
  29. Vengrenyuk Y, Carlier S, Xanthos S, et al. A hypothesis for

- vulnerable plaque rupture due to stress-induced debonding around cellular microcalcifications in thin fibrous caps. *Proc Natl Acad Sci U S A* 2006;103:14678-83.
30. Bluestein D, Alemu Y, Avrahami I, et al. Influence of microcalcifications on vulnerable plaque mechanics using FSI modeling. *J Biomech* 2008;41:1111-8.
  31. Cilla M, Monterde D, Peña E, et al. Does microcalcification increase the risk of rupture? *Proc Inst Mech Eng H* 2013;227:588-99.
  32. Huang H, Virmani R, Younis H, et al. The impact of calcification on the biomechanical stability of atherosclerotic plaques. *Circulation* 2001;103:1051-6.
  33. Maldonado N, Kelly-Arnold A, Vengrenyuk Y, et al. A mechanistic analysis of the role of microcalcifications in atherosclerotic plaque stability: potential implications for plaque rupture. *Am J Physiol Heart Circ Physiol* 2012;303:H619-28.
  34. Knésl Z, Klusák J, Náhlík L. Crack Initiation Criteria for Singular Stress Concentrations, Part I: A Universal Assessment of Singular Stress Concentrations. *Engineering Mechanics* 2007;14:399-40.
  35. Obaid DR, Calvert PA, McNab D, et al. Identification of coronary plaque sub-types using virtual histology intravascular ultrasound is affected by inter-observer variability and differences in plaque definitions. *Circ Cardiovasc Imaging* 2012;5:86-93.
  36. Huisman J, Egede R, Rdzanek A, et al. Between-centre reproducibility of volumetric intravascular ultrasound radiofrequency-based analyses in mild-to-moderate coronary atherosclerosis: an international multicentre study. *EuroIntervention* 2010;5:925-31.
  37. Murray SW, Palmer ND. What is behind the calcium? The relationship between calcium and necrotic core on virtual histology analyses. *Eur Heart J* 2009;30:125; author reply 125-6.
  38. Sales FJ, Falcao BA, Falcao JL, et al. Evaluation of plaque composition by intravascular ultrasound “virtual histology”: the impact of dense calcium on the measurement of necrotic tissue. *EuroIntervention* 2010;6:394-9.
  39. Obaid DR, Calvert PA, Gopalan D, et al. Atherosclerotic Plaque Composition and Classification Identified by Coronary Computed Tomography: Assessment of Computed Tomography-Generated Plaque Maps Compared with Virtual Histology Intravascular Ultrasound and Histology/Clinical Perspective. *Circ Cardiovasc Imaging* 2013;6:655-64.

**Cite this article as:** Murray SW, Patel B, Stables RH, Perry RA, Palmer ND. Site-specific intravascular ultrasound analysis of remodelling index and calcified necrosis patterns reveals novel blueprints for coronary plaque instability. *Cardiovasc Diagn Ther* 2014;4(4):287-298. doi: 10.3978/j.issn.2223-3652.2014.07.03